Structure parameters

Table S1. Structural parameters of the unit cell of $P6_3/m$ $HfIr_3B_4$.

Atom	X	Y	Z	Site
B	0.00000	0.00000	0.50000	2b
B	0.60246	0.55156	0.75000	6h
Hf	0.33333	0.66667	0.75000	2d
Ir	0.66762	0.74328	0.25000	6h

Computational Methods

In this study, the electronic structure of $P6_3/m$ $HfIr_3B_4$ was calculated using density functional theory, within the VASP code[1]. We also used the projector augmented wave (PAW)[2] method to deal with the interaction between the ion cores and valence electrons. The Perdew-Burke-Ernzerhof (PBE) parameterization of the generalized gradient approximation (GGA)[3] was selected to describe the exchange and correlation functionals. For the $HfIr_3B_4$ system, a plane-wave basis set cut-off of 500 eV and a Monkhorst-Pack special 5 × 5 × 9 k-point mesh were used in the Brillouin zone (BZ) integration. The unit cell was optimized until the force and total energy were less than 0.005 eV/Å and 0.0000001 eV, respectively. The surface states of $HfIr_3B_4$ were investigated in this study on a basis of a slab model built by *WannierTools*[4], according to the method of maximally localized Wannier functions[5]. The value of NSlab, i.e., Number of slabs for slab band was set as 20 in this work.

Band structure with MBJGGA

The MBJGGA functional possesses similar accuracy with more expensive functionals, such as HSE 06 and GW, in predicting the band order, and has been widely used in previous studies[6]. From Fig. S1, one can see that the MBJGGA calculation showed a similar band structure with GGA, where all the band crossing points (in R1, R2 and R3 regions) retained.

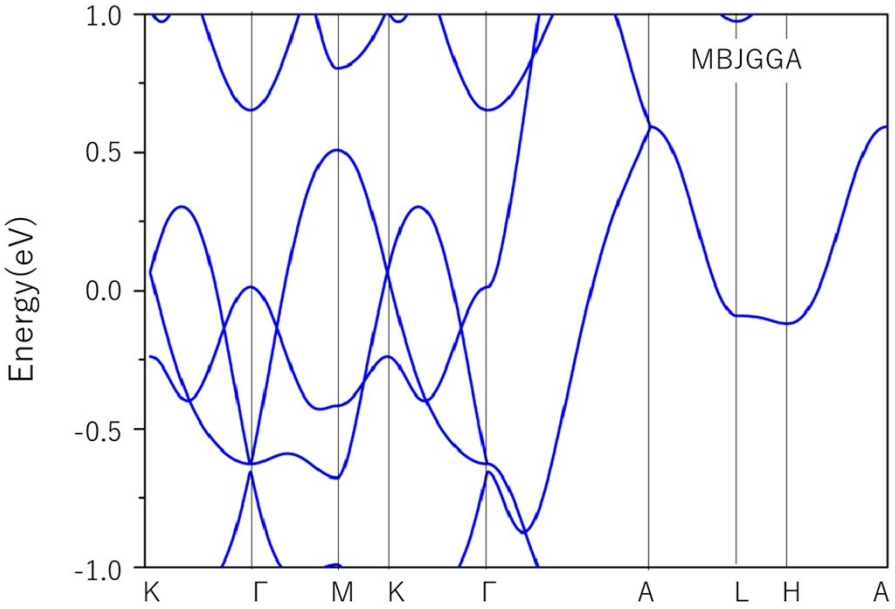

Fig. S1. Calculated band structure of $HfIr_3B_4$ with help of MBJGGA.

Calculated orbital-resolved band structure

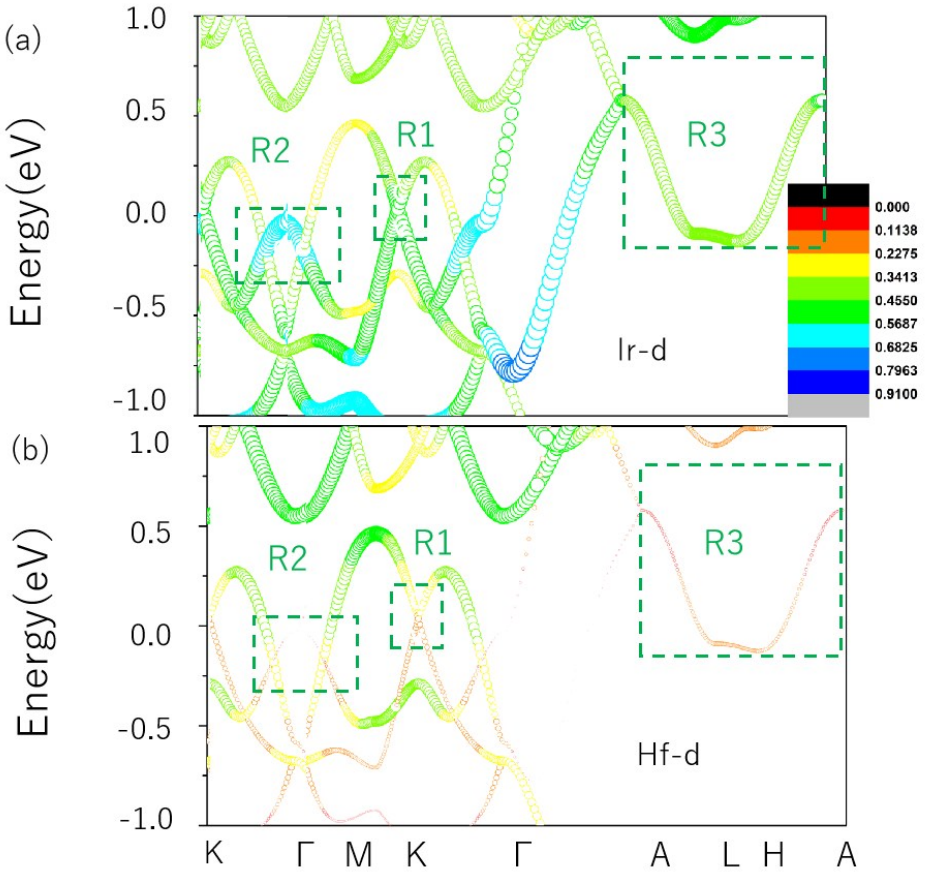

Fig. S2. Calculated orbital-resolved band structure of $HfIr_3B_4$.

Topological properties under the effect of spin-orbit coupling

The effect of SOC on the different TEs for $HfIr_3B_4$ is exhibited in Fig. S3. One can see that these TEs are very robust to the SOC effect. As shown in Fig. S3 (b) and Fig. S3 (c), no SOC-induced gaps can be found in R1 and R3 regions. However, for the topological nodal line (TNL) state in R2 region, indeed small SOC-induced gaps observed for both band crossing points. We would like to point out that $HfIr_3B_4$ can be regarded as a good topological semimetal hosts TNL in the k_z = 0 plane due to its gap sizes throughout the nodal line are less than 5 meV, which is much lower than typical TNLSs, such as ZrSiS (above 20 meV)[7], TiB_2 (above 25 meV)[8], Mg_3Bi_2 (above 36 meV)[9], and Cu_3PdN (above 60 meV)[10].

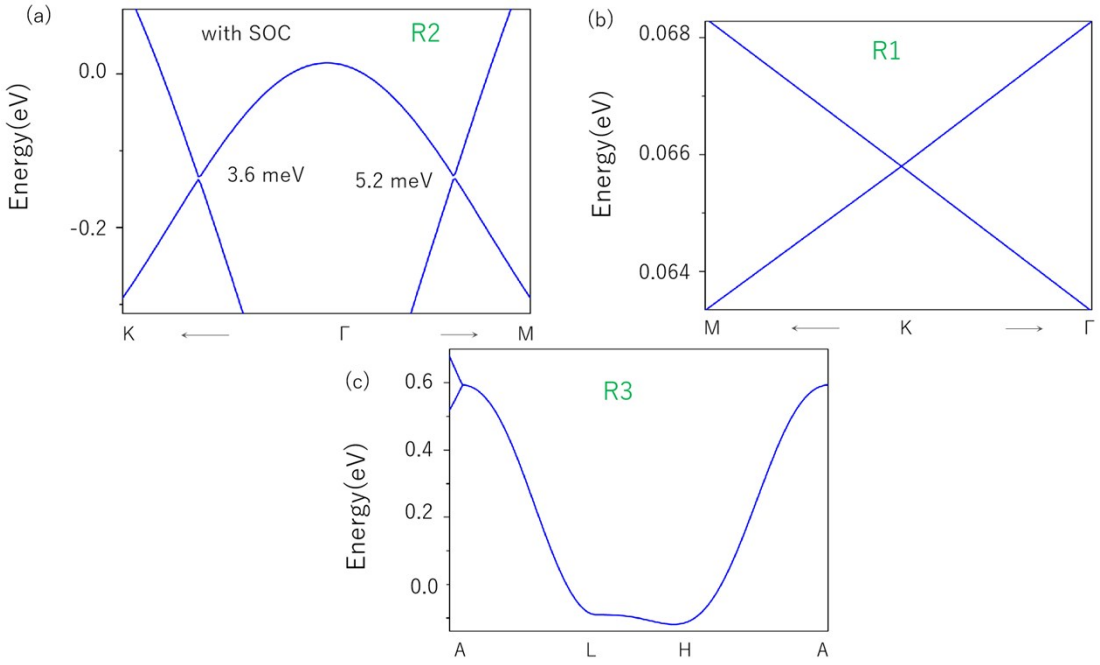

Fig. S3. Calculated band structure of $HfIr_3B_4$ in R1, R2, and R3 regions, with the SOC effect.

Electron and hole doping effects

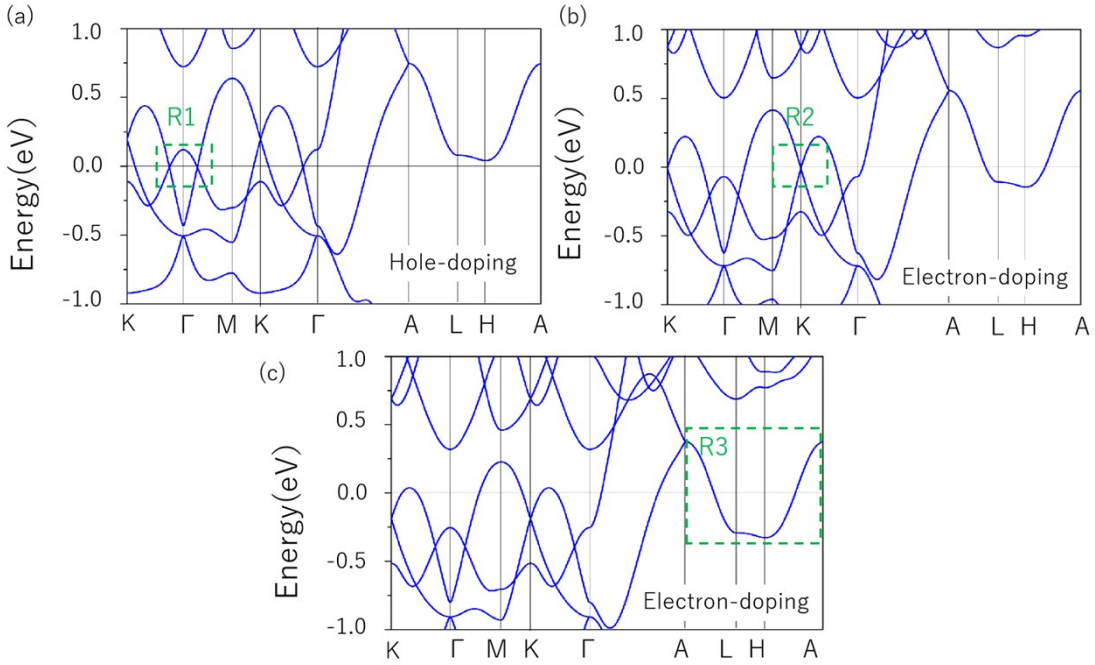

Fig. S4. Calculated band structures of $HfIr_3B_4$ under hole doping and electron doping effects: (a) with a hole doping concentration of 0.05 carrier per atom; (b) with an electron doping concentration of 0.0125 carrier per atom; (c) with an electron doping concentration of 0.05 carrier per atom.

References

[1] G. Kresse, J. Furthmüller, *Phys. Rev. B*, 1996, **54**, 169.

[2] P. E. Blöchl, *Phys. Rev. B*, 1994, **50**, 17953.

[3] J. P. Perdew, J. A. Chevary, S. H. Vosko, K. A. Jackson, M. R. Pederson, D. J. Singh, C. Fiolhais, *Phys. Rev. B*, 1992, **46**, 6671.

[4] Q. Wu, S. Zhang, H. Song, M. Troyer, A. Soluyanov, *Computer Phys. Commun.*, 2018, **224**, 405-416.

[5] N. Marzari, D. Vanderbilt, *Phys. Rev. B*, 1997, **56**, 12847.

[6] T. He, X. Zhang, W. Meng, L. Jin, X. Dai, G. Liu. *J. Mater. Chem. C*, 2019, **7(40)**, 12657-12663.

[7] M. Neupane, I. Belopolski, M. M. Hosen, *Phys. Rev. B*, 2016, **93**, 201104.

[8] X. Zhang, Z. M. Yu, X. L. Sheng, H. Y. Yang, S. A. Yang, *Phys. Rev. B*, 2017, **95**, 235116.

[9] X. Zhang, L. Jin, X. Dai, G. Liu, *J. Phys. Chem. Lett.*,2017, 8, 4814-4819.

[10] R. Yu, H. Weng, Z. Fang, X. Dai, X. Hu, *Phys. Rev. Lett.*, 2015, **115**, 036807.